Science World Journal Vol. 19(No 4) 2024 https://dx.doi.org/10.4314/swj.v19i4.31
www.scienceworldjournal.org
ISSN: 1597-6343 (Online), ISSN: 2756-391X (Print)
Published by Faculty of Science, Kaduna State University

Full Length Research Article

MATHEMATICAL MODELLING OF COVID-19 TRANSMISSION DYNAMICS IN KADUNA STATE, NIGERIA

*Danjuma Rose Uwanassara, Okolo Patrick Noah, Dauda Muhammad Kabir

Department of Mathematical Sciences, Kaduna State University, Kaduna, Nigeria

*Corresponding Author Email Address: roszypeterz1@gmail.com

ABSTRACT
This study developed a mathematical model of COVID-19 infection transmission dynamics incorporating asymptomatically and symptomatically-infectious individuals, the vital dynamics such as birth rate and mortality rate, face-mask use, diagnosis of asymptomatic infectious individuals, and isolation of infected individuals as control strategy are also incorporated. The model is shown to have two unique equilibrium states, namely: the disease-free and endemic equilibrium states, and the basic reproduction number was computed using the next generation matrix operator. The results obtained from the normalised forward sensitivity index show that the contact rate, face-mask efficacy and compliance, and isolation rate are the most influential factors on the spread of COVID-19 infectious disease. Numerical simulations show that, decreasing the infection transmission parameter will also reduce the size of the infective population. From the numerical simulations and results, it is recommended that a combination of decreasing contact rate, increasing face mask compliance and efficacy, clinical diagnosis of asymptomatic individuals, and isolation of symptomatic individuals is vital to public health strategy in eradicating COVID-19 infection and death in the shortest possible time.

Keywords: COVID-19, Positivity of Solution, Equilibrium States, Sensitivity Index, Basic Reproduction Number.

INTRODUCTION

The COVID-19 pandemic, caused by the novel severe acute respiratory syndrome coronavirus 2 (SARS-CoV-2), has created unprecedented public health and socioeconomic challenges worldwide. First identified in Wuhan, China, in December 2019 (Zhu *et al.,* 2020). On 12 Jan 2020, the Chinese authorities shared the sequence of a novel coronavirus termed the severe acute respiratory syndrome coronavirus 2 (SARS-CoV-2). Since then, the disease caused by SARS-CoV-2 has been named coronavirus disease 2019 (COVID-19) (Firas *et al.,* 2020). Due to human-human transmission, the number of infected people grew rapidly, forcing Wuhan to go into a strict lockdown. Since then, the pandemic has spread to over 210 countries, thereby inflicting severe public health and socio-economic burden in many parts of the world, including Nigeria. Nigeria, the most populous country in Africa, is one of the epicenters of COVID-19 in Africa. It has, as of 18 October 2021, accounted for over 209,298 confirmed cases, and 2,337 deaths (NCDC, 2021). Kaduna State in Northern Nigeria is also one of the most populous states in Nigeria. Like every other state in Nigeria, Kaduna State Government implemented measures such as the closing of schools, suspension of weekly church and mosque gatherings, the shutdown of sports centers, closing marketplaces, placing a curfew from 8 AM to 6 PM, closing inter-state borders and limiting the number of passengers in a commercial bus during intra-state travels. The virus rapidly spread globally, resulting in over 762 million confirmed cases and 6.8 million deaths as of April 2023 (WHO, 2023). Nigeria, as Africa's most populous nation, has faced significant burdens, with Kaduna State reporting over 9,901 confirmed cases and 78 deaths by October 2021 (NCDC, 2021).

According to Indwiana & Ysrafil (2020), COVID-19 is an infectious disease caused by a new coronavirus called SARS-CoV-2 which stands for Severe Acute Respiratory Syndrome Coronavirus 2. SARS-CoV-2 belongs to the beta subgrouping of the *coronaviridae* family and is an enveloped virus containing a positive-sense, single-stranded RNA with 29,891 bases of size. The genome encodes for 29 proteins involved in the infection, replication, and virion assembly process. The coronavirus gets its name from the crown-like spikes on its surface. Several types of coronaviruses can cause mild to severe respiratory illness, including the common cold, Middle East Respiratory Syndrome (MERS), and Severe Acute Respiratory Syndrome (SARS) (CDC, 2021).

The spike S protein from SARS-CoV-2 contains a receptor binding domain (RBD) that binds the human angiotensin-converting enzyme 2 (ACE2) and thereby, promotes membrane fusion and uptake of the virus into human cells by endocytosis. The RBD present in the spike protein is the most variable region of the coronavirus genome. Structural and biochemical studies have suggested that RBD from SARS-CoV-2 binds with high affinity to ACE2 compared to other SARS-CoV viruses, However, the human ACE2 protein variability may also be a factor for the high binding affinity. Because this virus is new, no one has any immunity to it. This means it will potentially infect

very large numbers of people (WHO, 2021).

From the time of exposure to COVID-19 infection to the moment when symptoms begin is on average 5-6 days and can range from 1-14 days (Li et al., 2020). According to WHO (2021), the most *common symptoms* of COVID-19 are Fever, dry cough, and fatigue. *Symptoms of severe* COVID-19 disease include loss of appetite, shortness of breath, confusion, persistent pain or pressure in the chest, and high temperature (above). People of all ages who experience fever and/or cough associated with difficulty in breathing, shortness of breath, chest pain or pressure, or loss of speech or movement should seek medical care immediately. Some people may experience severe illness, which can lead to hospitalisation and death (Guan *et al.,* 2020).

The primary mode of transmission is through respiratory droplets generated when an infected person talks, coughs, or sneezes. These droplets can land on nearby surfaces or directly on the mouth, nose, or eyes of another person nearby, leading to infection (CDC, 2022). As such, it is crucial to maintain physical distance, wear masks, and practise good hand hygiene to reduce the risk of transmission.

However, there is also evidence that the virus can be transmitted through aerosols, which are smaller particles that can remain suspended in the air for longer periods. Poorly ventilated indoor spaces, particularly those with limited air exchange or recirculation, increase the risk of airborne transmission (Zhang *et al.,* 2021). Proper ventilation and air filtration systems can help reduce the risk of airborne transmission in indoor environments. The COVID-19 pandemic has been a stark reminder of the importance of understanding how infectious diseases spread and taking the necessary precautions to prevent their transmission.

Several models have been formulated and analysed to explain the dynamics of COVID-19. Andrea *et al.* (2020) proposed the challenges of modelling and forecasting the spread of COVID-19. They insisted that modelling and forecasting the spread of COVID-19 remains a challenge, but they were able to present three macroscopic models, which include: Exponential growth model, the self-exciting branching process, and the SIR (susceptible-infected-resistant) compartmental model. Their study showed that addressing the coronavirus disease 2019 (COVID-19) outbreak will depend critically on the successful implementation of public health measures such as social distancing, shelter-in-place orders, disease surveillance, contact tracing, isolation, and quarantine.

Barbarossa *et al.* (2020) described modelling the spread of covid-19 in Germany, its early assessment, and possible scenarios. They simulated different possible strategies for the mitigation of the current outbreak which can help in slowing down the spread of the virus and thus, reduce the peak in daily diagnosed cases, the demand for hospital intensive care unit admissions, and eventually the number of fatalities. Their results suggested that a partial and gradual lifting of introduced control measures could soon be possible if accompanied by further increased testing activity, strict isolation of detected cases, and reduced contact with risk groups.

Tiwari (2020) investigated the modelling and analysis of covid-19 epidemic in India. Using the SIQR (susceptible-infectious-quarantined-recovered) model effective reproduction number, he was able to determine the epidemic doubling rate, and the infected-quarantined ratio was used to check the temporal evolution of the pandemic in India. He estimated that there is a strong positive correlation between testing rate and detection of new cases; up to 6 million tests per day.

Yuliya *et al*. (2020) developed mathematical modelling of the dynamics and containment of covid-19 in Ukraine. Their model included age-stratified disease parameters, as well as age-specific and location-specific contact matrices, to represent contacts. They showed that the model can provide an accurate short-term forecast for the numbers and age distribution of cases, and deaths. They also simulated different lockdown scenarios and the result suggested that reducing work contacts is more efficient at reducing the disease burden than reducing school contacts or implementing shielding for people over 60.

Daniel (2020) presented a mathematical model for the transmission of COVID-19 with nonlinear forces of infection and the need for prevention measures in Nigeria. She proposed a mathematical model, SEIQCRW (susceptible, exposed, infected, quarantined, confirmed, recovered, and virus) to study the current outbreak of COVID-19 in Nigeria with nonlinear forces of infection, considering the routes from the environment to humans and from human to human. The model defined the transmission channels in the infection dynamics and the impact of the environmental reservoir in the spread of this disease to humans. The study suggested washing hands, fumigation, etc. as helpful to control the transmission of the virus.

Enahoro *et al*. (2020) developed a mathematical model and analysis of the COVID-19 pandemic in Nigeria. The study showed that, in the absence of a safe and effective vaccine or antiviral for use against the pandemic in humans, control and efforts are focused on the use of non-pharmaceutical interventions (NPIs), community lockdown, contact tracing, quarantine of suspected cases, isolation of confirmed cases and the use of face masks in public. They also stated that relaxing or fully lifting the lockdown to re-open the economy or country might trigger a deadly second wave of the pandemic.

Yusuf *et al.* (2020) analysed mathematical modelling of covid-19 transmission and control strategies in the population of Bauchi State, Nigeria. This research work extended the epidemic SEIR model by introducing new parameters based on the transmission dynamics of the novel COVID-19 pandemic, which are: susceptible class, exposed class, infected class, quarantined class, and recovered class. The analysis and model

building was done using Maple software. They concluded by stating that contact tracing must be taken seriously because the models showed the rise in the infected class is a sign of the high vulnerability of the population and lack of vaccines. Unless quarantine is done adequately, despite the rate of recovery, the rate of infection will keep increasing in the absence of the COVID-19 vaccine at that moment.

Adewole *et al.* (2021) study showed how to model the dynamics of COVID-19 in Nigeria. They used Pontryagin's maximum principle to optimise the time-dependent intervention strategies to suppress the transmission of the virus. Numerical simulations were used to explore various optimal control solutions involving single and multiple controls. Also, sensitivity analysis was carried out to investigate the influence of the parameters in curtailing the disease. Their results suggested that a strict intervention effort is required, which involves identifying and isolating the infectious individuals to help reduce the spread of the disease.

Suleiman *et al.* (2021) presented an estimation of the case of COVID-19 epidemiological data in Nigeria using statistical regression analysis. They employed two statistical regression models, such as the linear and polynomial models to estimate the case fatality rate (CFR), based on the early phase of the Covid-19 outbreak in Nigeria. They recommended that the estimated CFR level of 0.03% in Nigeria will be maintained shortly only if there are no significant changes in the healthcare facilities, detection methods, continuous clinical treatments, and other factors. They also advised that the Government and relevant stakeholders should provide sufficient bed space and associated clinical care services to achieve a successful and effective control of COVID-19 in Nigeria.

Okolo *et al.,* (2021) developed a compartmental non-linear deterministic epidemic model of coronavirus information 2019 (COVID-19) transmission dynamics incorporating social distancing; face mask use and hospitalisation is formulated. The results of the sensitivity index show that the most sensitive parameter is the infection transmission probability which was also taken as the social distancing parameter. Numerical simulations show that using a single intervention strategy is beneficial in reducing the COVID-19 disease burden. It is further demonstrated that the effective combination of social distancing, use of face masks in public, and isolation (hospitalisation) of infected individuals will lead to a great disease in COVID-19 infection burden.

Mathematical models have been critical tools for understanding the transmission dynamics of infectious diseases and evaluating intervention strategies. Various studies have explored the dynamics of COVID-19 using compartmental models such as SEIR, SIQR, and other extensions (Tiwari, 2020; Yusuf et al., 2020). However, many existing models fail to account for key factors such as population demography (birth and death rates), clinical diagnosis of asymptomatic cases, and the impact of localised interventions of face-mask compliance and isolation measures. Furthermore, limited research focuses on COVID-19 dynamics in specific Nigerian states, such as Kaduna, despite the unique demographic and epidemiological factors.

This study aims to address these gaps by extending Danjuma et al., (2023) model, incorporating vital dynamics, a proportion of the population that uses face-mask, the efficacy of face masks, the effect of isolating infected individuals, and the impact of clinical diagnosis of the asymptomatically-infectious individuals. Using confirmed COVID-19 data from Kaduna State, the model evaluates the effectiveness of various control measures in reducing COVID-19 transmission. The findings provide insights for public health policymakers in managing infectious disease outbreaks.

MATERIALS AND METHODS

The Models

The total human population at time t denoted by $N(t)$ is divided into six mutually-exclusive compartments of Susceptible $(S(t))$, Exposed $(E(t))$, Asymptomatically-infectious $(I_a(t))$, Symptomatically-infectious $(I(t))$, Isolated $(I_s(t))$ and Recovered $(R(t))$ individuals, so that,

$$N(t) = S(t) + E(t) + I_A(t) + I(t) + I_s(t) + R(t) \quad (*)$$

The variables and parameters used in the model are defined in Table 1.

Table 1: Description of variables and parameters

Variables / Parameters	Description
$S(t)$	Number of Susceptible individuals at a given time *t.*
$E(t)$	Number of Exposed individuals at a given time *t.*
$I_A(t)$	Number of Asymptomatic individuals at a given time *t.*
$I(t)$	Number of Symptomatic individuals at a given time *t.*
$I_S(t)$	Number of Isolated individuals at a given time *t.*
$R(t)$	Number of Recovered individuals at a given time *t.*
Π	The population influx rate.
β	Infection transmission rate.
θ	Proportion of individuals who wear face-masks in public.
q	Efficacy of face-masks.
η	The rate at which the asymptomatic individuals develop symptoms as a result of clinical diagnosis.
v	The isolation rate for symptomatic-infectious individuals.
σ	The proportion of exposed individuals who show no clinical symptoms.

Science World Journal Vol. 19(No 4) 2024 https://dx.doi.org/10.4314/swj.v19i4.31
www.scienceworldjournal.org
ISSN: 1597-6343 (Online), ISSN: 2756-391X (Print)
Published by Faculty of Science, Kaduna State University

ω	The rate of progression from the exposed compartment to the infectious compartment.
γ	The recovery rate for individuals asymptomatically-infected, symptomatically-infected and isolated compartments.
d	The COVID-19 fatality rate of the asymptomatically-infected, symptomatically-infected and isolated class.
μ	Natural death rate.

From the above description of variables and parameters, the interaction and flow in the different compartments are as depicted in the schematic diagram below in Figure 1**.**

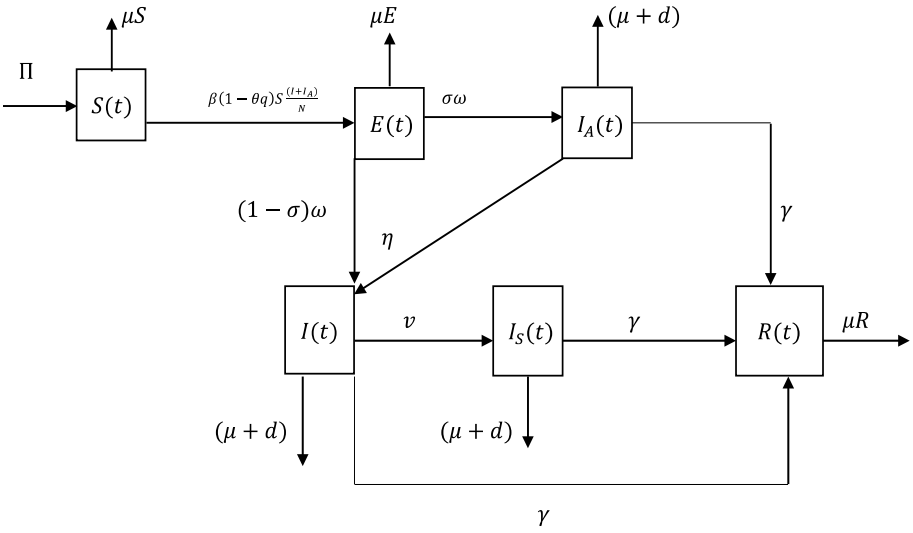

Figure 1: Schematic diagram of COVID-19 transmission dynamics.

The Model Equations

The above assumptions and formulations lead to the following system of ordinary differential equations:

$$\frac{dS}{dt} = \Pi - \beta(1-\theta q)S\frac{(I+I_A)}{N} - \mu S \quad (1)$$

$$\frac{dE}{dt} = \beta(1-\theta q)S\frac{(I+I_A)}{N} - (\omega+\mu)E \quad (2)$$

$$\frac{dI_A}{dt} = \sigma\omega E - (\gamma+\eta+\mu+d)I_A \quad (3)$$

$$\frac{dI}{dt} = (1-\sigma)\omega E + \eta I_A - (\gamma+v+\mu+d)I \quad (4)$$

$$\frac{dI_s}{dt} = vI - (\gamma+\mu+d)I_s \quad (5)$$

$$\frac{dR}{dt} = \gamma I_A + \gamma I + \gamma I_s - \mu R \quad (6)$$

with the non-negative initial condition $S(0) = S_0 > 0, E(0) = E_0 > 0, I_A(0) = I_{A_0} > 0, I(0) = I_0 > 0, I_s(0) = I_{S_0} > 0, R(0) = R_0 > 0$ (7)

Invariant Region

Consider the biologically feasible region

$$\Omega = \left\{\left(S(t), E(t), I_A(t), I(t), I_s(t), R(t)\right) \in \mathbb{R}^6 : N \leq \frac{\pi}{\mu}\right\} \quad (8)$$

Lemma 2.1: The closed set Ω is positively invariant and attracting with respect to the system equations (1) – (6).

Proof:

Adding equation (1) – (6) gives the rate of change of the total population

$$\frac{dN}{dt} = \Pi - \mu N - d(I_A + I + I_s) \quad (9)$$

It is clear from the equation (10) that

$$\frac{dN}{dt} \leq \Pi - \mu N \quad (10)$$

it follows that

Science World Journal Vol. 19(No 4) 2024 https://dx.doi.org/10.4314/swj.v19i4.31
www.scienceworldjournal.org
ISSN: 1597-6343 (Online), ISSN: 2756-391X (Print)
Published by Faculty of Science, Kaduna State University

$$\frac{dN}{dt} \leq 0, \qquad \text{if } N(t) \geq \frac{\Pi}{\mu}$$

Thus, by a standard comparison theorem (Lakshmikantham *et al.,* 1989) can be used to show that

$$N(t) = N(0)e^{-\mu t} + \frac{\Pi}{\mu}(1 - e^{-\mu t}) \qquad (11)$$

In particular,

$$N(t) \leq \frac{\Pi}{\mu} \quad \text{if} \quad N(0) \leq \frac{\Pi}{\mu}$$

Thus, the region $\Omega = \{(S, E, I_A\, I, I_S, R) \in \mathbb{R}^6 : N \leq \frac{\pi}{\mu}\}$ is positively invariant. However, if $N(t) \leq \frac{\Pi}{\mu}$, then either the solution enters Ω in a finite time, or $N(t)$ approaches $\frac{\Pi}{\mu}$ asymptotically. Hence, the region Ω attracts all solutions in $\mathbb{R}^6$.

Therefore, it is sufficient to consider the dynamics of the flow generated by equations (1) – (6) in Ω where the usual existence, uniqueness, and continuation results hold for the system (1) – (6), that is, the system is mathematically and epidemiologically well-posed in Ω.

Model Analysis

Disease-Free Equilibrium (DFE) Point

The Disease-Free Equilibrium (DFE) state of the model (1) – (6) , $\mathcal{E}_0$ is given as:

$$\mathcal{E}_0 = (S_0, 0, 0, 0, 0, 0) = \left(\frac{\Pi}{\mu}, 0, 0, 0, 0, 0\right) \qquad (12)$$

To assess the stability of COVID-19, the computation of the basic reproduction number R_0 is needed.

Basic Reproduction Number (R_0)

The basic reproduction number of an infectious disease is the average of secondary infections when one infected individual is introduced into a host population where everyone is susceptible (Diekmann, *et al.,* 1990; Van Den Driessche & Watmough, 2002). We use the next-generation matrix approach to compute the basic reproduction number R_0. The basic reproduction number R_0 is the spectral radius of the product matrix FV^{-1}. That is,

$$R_0 = \sigma(FV^{-1}) \qquad (13)$$

where σ denotes the spectral radius.

The associated non-negative matrix F, for the new infective terms and the non-singular M-matrix, V, for the remaining transfer terms at the DFE are respectively given by

$$F_x(\mathcal{E}_0) = \begin{pmatrix} 0 & \beta(1-\theta q)\frac{\Pi}{\mu N} & \beta(1-\theta q)\frac{\Pi}{\mu N} \\ 0 & 0 & 0 \\ 0 & 0 & 0 \end{pmatrix} \qquad (14)$$

and

$$V = \begin{pmatrix} (\omega+\mu) & 0 & 0 \\ -\sigma\omega & (\gamma+\eta+\mu+d) & 0 \\ -(1-\sigma)\omega & -\eta & (\gamma+v+\mu+d) \end{pmatrix} \qquad (15)$$

$$V_x^{-1} = \begin{pmatrix} \frac{1}{(\omega+\mu)} & 0 & 0 \\ \frac{\sigma\omega}{a_1(\omega+\mu)} & \frac{1}{a_1} & 0 \\ \frac{\eta\sigma\omega + a_1(1-\sigma)\omega}{a_1 a_2(\omega+\mu)} & \frac{\eta}{a_1 a_2} & \frac{1}{a_2} \end{pmatrix} \qquad (16)$$

where,

$$a_1 = (\gamma+\eta+\mu+d)$$
$$a_2 = (\gamma+v+\mu+d)$$

so that

$$F_x V_x^{-1} = \begin{pmatrix} \beta(1-\theta q)\frac{\Pi}{\mu N}\left[\frac{\sigma\omega}{a_1(\omega+\mu)}\right] + \beta(1-\theta q)\frac{\Pi}{\mu N}\left[\frac{\eta\sigma\omega + a_1(1-\sigma)\omega}{a_1 a_2(\omega+\mu)}\right] & \beta(1-\theta q)\frac{\Pi}{\mu N}\left[\frac{1}{a_2}\right] + \beta(1-\theta q)\frac{\Pi}{\mu N}\left[\frac{\eta}{a_1 a_2}\right] & \beta(1-\theta q)\frac{\Pi}{\mu N}\left[\frac{1}{a_1}\right] \\ 0 & 0 & 0 \\ 0 & 0 & 0 \end{pmatrix} \qquad (17)$$

$$J(\mathcal{E}_0) = \begin{pmatrix} -\mu & 0 & -\beta(1-\theta q)\frac{\Pi}{\mu N} & -\beta(1-\theta q)\frac{\Pi}{\mu N} & 0 & 0 \\ 0 & -(\omega+\mu) & \beta(1-\theta q)\frac{\Pi}{\mu N} & \beta(1-\theta q)\frac{\Pi}{\mu N} & 0 & 0 \\ 0 & \sigma\omega & -(\gamma+\eta+\mu+d) & 0 & 0 & 0 \\ 0 & (1-\sigma)\omega & \eta & -(\gamma+v+\mu+d) & 0 & 0 \\ 0 & 0 & 0 & v & -(\gamma+\mu+d) & 0 \\ 0 & 0 & \gamma & \gamma & \gamma & -\mu \end{pmatrix} \qquad (19)$$

It follows that the basic reproduction number, denoted by R_0, given by $\sigma(FV^{-1})$ where σ denotes the spectral radius is

$$\mathcal{R}_0 = \frac{\beta(1-\theta q)\Pi}{\mu \mathrm{N}(\omega+\mu)}\left[\frac{\sigma\omega}{a_1} + \frac{\eta\sigma\omega + a_1(1-\sigma)\omega}{a_1 a_2}\right] \qquad (18)$$

Local Stability of Disease Free Equilibrium (DFE) State

We investigated the local stability of the Disease-Free Equilibrium (DFE) state by evaluating the associated Jacobian of equations (1) – (6) at the DFE state. The Jacobian matrix J the system (1) – (6), evaluated at the disease-free equilibrium, $J(\mathcal{E}_0)$ is given by

Theorem 3.1: The DFE state of the model (1) – (6) given by $\mathcal{E}_0$, is locally asymptotically stable whenever $R_0 < 1$ and $\mathcal{E}_0$ is unstable if $R_0 > 1$.

Proof:

It suffices to show that all the eigenvalues of the characteristics equation of the Jacobian matrix $J(\mathcal{E}_0)$, have negative real parts. The eigenvalues are determined by solving the characteristics equation $\det(J(\mathcal{E}_0) - \lambda I) = 0$

Science World Journal Vol. 19(No 4) 2024 https://dx.doi.org/10.4314/swj.v19i4.31
www.scienceworldjournal.org
ISSN: 1597-6343 (Online), ISSN: 2756-391X (Print)
Published by Faculty of Science, Kaduna State University

Evaluating equation (19) to obtain,

$$(-\mu-\lambda)(-\mu-\lambda)(-a_3-\lambda)\begin{vmatrix} -(\omega+\mu)-\lambda & \beta(1-\theta q)\frac{\Pi}{\mu N} & \beta(1-\theta q)\frac{\Pi}{\mu N} \\ \sigma\omega & -a_1-\lambda & 0 \\ (1-\sigma)\omega & \eta & -a_2-\lambda \end{vmatrix}=0$$

where,

$$a_1=(\gamma+\eta+\mu+d)$$
$$a_2=(\gamma+\nu+\mu+d)$$
$$a_3=(\gamma+\mu+d)$$

Simplifying to obtain

$$(-\mu-\lambda)\ \ (-\mu-\lambda)(-a_3-\lambda)\ \ \Big[\lambda^3+\lambda^2(a_1+a_2+\ \omega+\mu)+\lambda\Big[-\beta(1-\theta q)\frac{\Pi\sigma\omega}{\mu N}-\beta(1-\theta q)\frac{\Pi(1-\sigma)\omega}{\mu N}+a_1a_2+(a_1+a_2)(\omega+\mu)\Big]-\beta(1-\theta q)\frac{\Pi}{\mu N}[\eta\sigma\omega+a_1\omega-a_1\sigma\omega+a_2\sigma\omega]+a_1a_2(\omega+\mu)\Big]=0 \quad (20)$$

Thus, the eigenvalues are: $\lambda=-\mu$ (twice), $\lambda=-a_3$ and the polynomial $\lambda^3+A\lambda^2+B\lambda+C=0$
where,

$$A=a_1+a_2+\ \omega+\mu, \quad (21)$$

$$B=a_1a_2+a_1(\omega+\mu)+a_2(\omega+\mu)-\beta(1-\theta q)\frac{\Pi\sigma\omega}{\mu N}-\beta(1-\theta q)\frac{\Pi(1-\sigma)\omega}{\mu N}, \quad (22)$$

$$C=-\frac{\beta(1-\theta q)\frac{\Pi}{\mu N}}{(\omega+\mu)}\left[\frac{\eta\sigma\omega+a_1(1-\sigma)\omega}{a_1a_2}+\frac{\sigma\omega}{a_1}\right]+a_1a_2(\omega+\mu), \quad (23)$$

The Routh-Hurwitz stability (Routh-Hurwitz, 1964) criteria could be used to determine the sign of the eigenvalues. By the Routh-Hurwitz criteria, all the roots of the characteristics equation (20) have negative real parts if: $A,B,C>0, AB-C>0$
Obviously,

$$A=a_1+a_2+\ \omega+\mu\ >\ 0$$

$$B=a_1a_2+a_1(\omega+\mu)\Big[1-R_0+\Big(\frac{\beta(1-\theta q)\Pi\sigma\eta\omega}{a_1a_2(\omega+\mu)\mu N}+\frac{\beta(1-\theta q)\Pi(1-\sigma)\omega}{a_2(\omega+\mu)\mu N}\Big)\Big]+a_2(\omega+\mu)\Big[1-R_0+\Big(\frac{\beta(1-\theta q)\Pi\sigma\omega}{a_1(\omega+\mu)\mu N}+\frac{\beta(1-\theta q)\Pi\sigma\eta\omega}{a_1a_2(\omega+\mu)\mu N}\Big)\Big]>0, if\ R_0<1$$

$$C=\ a_1a_2(\omega+\mu)\Big[1-R_0+\Big(\frac{\beta(1-\theta q)\Pi\sigma\omega}{a_1(\omega+\mu)\mu N}+\frac{\beta(1-\theta q)\Pi\sigma\eta\omega}{a_1a_2(\omega+\mu)\mu N}+\frac{\beta(1-\theta q)\Pi(1-\sigma)\omega}{a_2(\omega+\mu)\mu N}\Big)\Big]>0, if\ R_0<1$$

Thus, $=a_1^2a_2+a_1^2(\omega+\mu)\Big[1-R_0+\Big(\frac{\beta(1-\theta q)\Pi\sigma\eta\omega}{a_1a_2(\omega+\mu)\mu N}+\frac{\beta(1-\theta q)\Pi(1-\sigma)\omega}{a_2(\omega+\mu)\mu N}\Big)\Big]++a_1a_2(\omega+\mu)\Big[1-R_0+\Big(\frac{\beta(1-\theta q)\Pi\sigma\omega}{a_1(\omega+\mu)\mu N}+\frac{\beta(1-\theta q)\Pi\sigma\eta\omega}{a_1a_2(\omega+\mu)\mu N}\Big)\Big]+a_1a_2^2+a_1a_2(\omega+\mu)\Big[1-R_0+\Big(\frac{\beta(1-\theta q)\Pi\sigma\eta\omega}{a_1a_2(\omega+\mu)\mu N}+\frac{\beta(1-\theta q)\Pi(1-\sigma)\omega}{a_2(\omega+\mu)\mu N}\Big)\Big]+a_2^2(\omega+\mu)\Big[1-R_0+\Big(\frac{\beta(1-\theta q)\Pi\sigma\omega}{a_1(\omega+\mu)\mu N}+\frac{\beta(1-\theta q)\Pi\sigma\eta\omega}{a_1a_2(\omega+\mu)\mu N}\Big)\Big]+a_1a_2(\omega+\mu)+a_1(\omega+\mu)^2\Big[1-R_0+\Big(\frac{\beta(1-\theta q)\Pi\sigma\eta\omega}{a_1a_2(\omega+\mu)\mu N}+\frac{\beta(1-\theta q)\Pi(1-\sigma)\omega}{a_2(\omega+\mu)\mu N}\Big)\Big]+a_2(\omega+\mu)^2\Big(\frac{\beta(1-\theta q)\Pi\sigma\omega}{a_1(\omega+\mu)\mu N}+\frac{\beta(1-\theta q)\Pi\sigma\eta\omega}{a_1a_2(\omega+\mu)\mu N}\Big)-a_1a_2(\omega+\mu)+a_1a_2(\omega+\mu)R_0>0,$ if $R_0<1$ (24)

Global Stability of Disease-Free Equilibrium (DFE) State

To ensure that COVID-19 infection eradication is independent of the initial size of the population of the model, it is imperative to show that the DFE of the model (1) – (6) given by $\mathcal{E}_0$ is globally asymptotically stable (GAS). To achieve this, we will use the following results introduced by (Castillo-Chavez et al, 2002).

Lemma 3.1: (Castillo-Chavez et al, 2002). Let systems of equation (1) – (6) be written in the form:

$$\frac{dX}{dt}=W(X,Y) \quad (25)$$

$$\frac{dY}{dt}=G(X,Y), \qquad G(X,0)=0 \quad (26)$$

where $X\in\mathbb{R}^m$ denotes (its components), the number of uninfected individuals and $Y\in\mathbb{R}^n$ denotes (its components), the number of infected individuals including latent, infectious, etc. $X_0=(X^*,0)$ denotes the DFE of the system. Also assume the conditions H_1 and H_2 below:

(H_1) for $\frac{dX}{dt}=W(X,0), X^*$ is globally asymptotically stable (GAS),

(H_2) for $G(X,Y)=QY-\hat{G}(X,Y), \hat{G}(X,Y)\geq 0$ for $(X,Y)\in\Omega$,

where the Jacobian $Q=\left(\frac{\partial G}{\partial Y}\right)_{X_0}$ is an Metzler matrix (M-matrix, for off-diagonal elements of Q are non-negative) and Ω is the region where the model makes biological sense. Then the DFE, $X_0=(X^*,0)$ is globally asymptotically stable provided that $R_0<1$. If the system satisfies these two conditions, then the following lemma holds.

Lemma 3.2: *The disease free equilibrium $X_0=(X^*,0)$ of the system of equations (1) - (6) is globally asymptotically stable (GAS) provided that $R_0<1$ and the assumptions H_1 and H_2 are satisfied.*

Now, we state the following theorem.

Theorem 3.2: The disease-free equilibrium of the system of equations (1) – (6) is globally asymptotically stable if $R_0<1$.

Proof: We adopt the notations in Lemma 3.2 and verify the conditions (H_1) and (H_2).

In our model, $X=(S,R)^T$, $Y=(E,I_A,I,I_S)$, and $X^*=$

Science World Journal Vol. 19(No 4) 2024 https://dx.doi.org/10.4314/swj.v19i4.31
www.scienceworldjournal.org
ISSN: 1597-6343 (Online), ISSN: 2756-391X (Print)
Published by Faculty of Science, Kaduna State University

$(\frac{\pi}{\mu}, 0)$.
The uninfected subsystem is:

$$\frac{d}{dt}\begin{bmatrix}S\\R\end{bmatrix} = W = \begin{bmatrix}\Pi - \beta(1-\theta q)S\frac{(I+I_A)}{N} - \mu S\\ Y(I_A + I + I_S) - \mu R\end{bmatrix} \quad (27)$$

When $E = I_A = I = I_S = 0$, the uninfected subsystem (27) becomes,

$$\frac{d}{dt}\begin{bmatrix}S\\R\end{bmatrix} = \begin{bmatrix}\Pi - \mu S\\ -\mu R\end{bmatrix} \quad (28)$$

and its solution is,

$$R(t) = R(0)e^{-\mu t}, S(t) = S(0)e^{-\mu t} + \frac{\Pi}{\mu}(1 - e^{-\mu t})$$

clearly, $R(t) \longrightarrow 0 \; and \; S(t) \longrightarrow \frac{\Pi}{\mu} \; as \; t \longrightarrow \infty$,
regardless of the values of $R(0) \; and \; S(0)$. Hence, $X^* = (\frac{\Pi}{\mu}, 0)$ is globally asymptotically stable for the subsystem.

$$\frac{dX}{dt} = W(X, 0)$$

Next, we have

$$Q = \begin{pmatrix} -(\omega+\mu) & \beta(1-\theta q)\frac{\Pi}{\mu N} & \beta(1-\theta q)\frac{\Pi}{\mu N} & 0 \\ \sigma\omega & -(\gamma+\eta+\mu+d) & 0 & 0 \\ (1-\sigma)\omega & \eta & -(\gamma+v+\mu+d) & 0 \\ 0 & 0 & v & -(\gamma+\mu+d) \end{pmatrix} \quad (29)$$

From $G(X,Y) = QY - \hat{G}(X,Y)$

$$\hat{G}(X,Y) = QY - G(X,Y)$$

$$\begin{pmatrix} -(\omega+\mu) & \beta(1-\theta q)\frac{\Pi}{\mu N} & \beta(1-\theta q)\frac{\Pi}{\mu N} & 0 \\ \sigma\omega & -(\gamma+\eta+\mu+d) & 0 & 0 \\ (1-\sigma)\omega & \eta & -(\gamma+v+\mu+d) & 0 \\ 0 & 0 & v & -(\gamma+\mu+d) \end{pmatrix} \begin{pmatrix} E \\ I_A \\ I \\ I_S \end{pmatrix} - \begin{pmatrix} \beta(1-\theta q)\frac{\Pi}{\mu N}(I_A + I) - (\omega+\mu)E \\ \sigma\omega E - (\gamma+\eta+\mu+d)I_A \\ (1-\sigma)\omega E + \eta I_A - (\gamma+v+\mu+d)I \\ vI - (\gamma+\mu+d)I_S \end{pmatrix} \quad (30)$$

$$\hat{G}(X,Y) = \begin{pmatrix} \beta(1-\theta q)\frac{(I+I_A)}{N}\left[\frac{\Pi}{\mu} - S\right] \\ 0 \\ 0 \\ 0 \end{pmatrix} \quad (31)$$

It is clear that $\hat{G}(X,Y) \geq 0$ for all $(X,Y) \in \Omega$. We also note that G is an M-Matrix since its off-diagonal elements are non-negative. Based on **Lemma 3.2**, the DFE $\mathcal{E}_0 = (\frac{\Pi}{\mu}, 0,0,0,0)$ is globally asymptotically stable when $R_0 < 1$.

Existence & Local Stability Analysis of the Endemic Equilibrium (EE) State

We investigated the local stability of the Endemic Equilibrium (EE) state by evaluating the associated Jacobian of equations (1) – (6) at the EE state. The Jacobian matrix J the system (1) – (6), evaluated at the endemic equilibrium, $J(\mathcal{E}_1)$ is given by

$$J(\mathcal{E}_1) = \begin{pmatrix} -\beta(1-\theta q)\frac{(I^*+I_A^*)}{N} - \mu & 0 & -\beta(1-\theta q)\frac{S^*}{N} & -\beta(1-\theta q)\frac{S^*}{N} & 0 & 0 \\ \beta(1-\theta q)\frac{(I^*+I_A^*)}{N} & -(\omega+\mu) & \beta(1-\theta q)\frac{S^*}{N} & \beta(1-\theta q)\frac{S^*}{N} & 0 & 0 \\ 0 & \sigma\omega & -(\gamma+\eta+\mu+d) & 0 & 0 & 0 \\ 0 & (1-\sigma)\omega & \eta & -(\gamma+v+\mu+d) & 0 & 0 \\ 0 & 0 & 0 & v & -(\gamma+\mu+d) & 0 \\ 0 & 0 & \gamma & \gamma & \gamma & -\mu \end{pmatrix}$$

Theorem 3.3: The EE state of the model (1) – (6) given by $\mathcal{E}_1$, is locally asymptotically stable whenever $R_0 > 1$.

Proof:

It suffices to show that all the eigenvalues of the characteristics equation of the Jacobian matrix $J(\mathcal{E}_1)$, have negative real parts. The eigenvalues are determined by solving the characteristics equation $\det(J(\mathcal{E}_1) - \lambda I) = 0$

$$\begin{vmatrix} -\beta(1-\theta q)\frac{(I^*+I_A^*)}{N} - \mu - \lambda & 0 & -\beta(1-\theta q)\frac{S^*}{N} & -\beta(1-\theta q)\frac{S^*}{N} & 0 & 0 \\ \beta(1-\theta q)\frac{(I^*+I_A^*)}{N} & -(\omega+\mu) - \lambda & \beta(1-\theta q)\frac{S^*}{N} & \beta(1-\theta q)\frac{S^*}{N} & 0 & 0 \\ 0 & \sigma\omega & -a_1 - \lambda & 0 & 0 & 0 \\ 0 & (1-\sigma)\omega & \eta & -a_2 - \lambda & 0 & 0 \\ 0 & 0 & 0 & v & -a_3 - \lambda & 0 \\ 0 & 0 & \gamma & \gamma & \gamma & -\mu - \lambda \end{vmatrix} = 0 \quad (32)$$

$$a_1 = (\gamma + \eta + \mu + d),$$
$$a_2 = (\gamma + v + \mu + d),$$
$$a_3 = (\gamma + \mu + d),$$

Evaluating equation (32) to obtain,

$$(-\mu - \lambda)(-a_3 - \lambda)\begin{vmatrix} a_4 - \mu - \lambda & 0 & b & b \\ -a_4 & -(\omega+\mu) - \lambda & -b & -b \\ 0 & \sigma\omega & -a_1 - \lambda & 0 \\ 0 & (1-\sigma)\omega & \eta & -a_2 - \lambda \end{vmatrix} = 0 \quad (33)$$

where,

$$b = \frac{-a_1 a_2(\omega+\mu)}{[(1-\sigma)\omega a_2 + \eta\sigma\omega + \sigma\omega a_1]},$$

$$a_4 = \frac{\beta(1-\theta q)}{N}\left[\frac{\sigma\omega}{a_2} + \frac{(1-\sigma)\omega a_2 + \eta\sigma\omega}{a_1 a_2}\right]\frac{\Pi}{(\omega+\mu)R_0}[1 - R_0]$$

Simplifying to have,

$(-\mu-\lambda)\;(-a_3-\lambda)\,[\lambda^4 + [(\omega+\mu) + (a_1+a_2) + \mu - a_4)]\lambda^3 + [(\omega+\mu)(a_1+a_2) + a_1a_2 + b\sigma\omega + \mu(\omega+\mu) + \mu(a_1+a_2) - a_4(\omega+\mu) + (a_1+a_2)]\lambda^2 + [(\omega+\mu)a_1a_2 + b\sigma\omega a_2 + b\sigma\omega\eta + b(1-\sigma)\omega a_2 + \mu((\omega+\mu)(a_1+a_2)) + a_1a_2 + b\sigma\omega - a_4((\omega+\mu)(a_1+a_2) + a_1a_2 + b\sigma\omega) + b(\sigma\omega + (1-\sigma)\omega + a_4\sigma\omega + a_4(1-\sigma)\omega]\lambda + [\mu(\omega+\mu)a_1a_2 + b\sigma\omega a_2 + b\sigma\omega\eta + b(1-\sigma)\omega a_2 - a_4[b\sigma\omega a_2 + b\sigma\omega\eta + b(1-\sigma)\omega a_2 + (\omega+\mu)a_1a_2] + b(\sigma\omega a_2 + \sigma\omega\eta + (1-\sigma)\omega a_1 + a_4\sigma\omega a_2 + a_4\sigma\omega\eta + a_4(1-\sigma)\omega a_1 = 0$ (34)

Thus, the eigenvalues are $\lambda_1 = -\mu, \lambda_2 = -a_3$ and the fourth-order polynomial

$\lambda^4 + A\lambda^3 + B\lambda^2 + C\lambda + D = 0$

where,

$$A = (\omega+\mu)+(a_1+a_2)+\mu-a_4)$$

$$A = (\omega+\mu)+(a_1+a_2)+\mu + \frac{\beta(1-\theta q)}{N}\left[\frac{\sigma\omega}{a_2}+\frac{(1-\sigma)\omega a_2+\eta\sigma\omega}{a_1a_2}\right]\frac{\Pi}{(\omega+\mu)R_0}[R_0-1] > 0 \; if \; R_0 > 1 \quad (35)$$

$$B = (\omega+\mu)(a_1+a_2)+a_1a_2+\mu(\omega+\mu)+\mu(a_1+a_2) + \frac{\beta(1-\theta q)}{N}\left[\frac{\sigma\omega}{a_2} + \frac{(1-\sigma)\omega a_2+\eta\sigma\omega}{a_1a_2}\right]\frac{\Pi}{(\omega+\mu)R_0}[R_0 - 1](\omega+\mu)+(a_1+a_2)] - \frac{a_1a_2(\omega+\mu)\sigma\omega}{[(1-\sigma)\omega a_2+\eta\sigma\omega+\sigma\omega a_1]} \; if \; R_0 > 1 \quad (36)$$

$$C = (\omega+\mu)a_1a_2 + \frac{\beta(1-\theta q)}{N}\left[\frac{\sigma\omega}{a_2}+\frac{(1-\sigma)\omega a_2+\eta\sigma\omega}{a_1a_2}\right]\frac{\Pi}{(\omega+\mu)R_0}[R_0 - 1]\big((\omega+\mu)(a_1+a_2)+a_1a_2\big)\big)+\mu\big((\omega+\mu)(a_1+a_2)+a_1a_2\big) + \frac{\beta(1-\theta q)}{N}\left[\frac{\sigma\omega}{a_2}+\frac{(1-\sigma)\omega a_2+\eta\sigma\omega}{a_1a_2}\right]\frac{\Pi}{(\omega+\mu)R_0}[R_0 - 1]\left[\frac{a_1a_2(\omega+\mu)}{[(1-\sigma)\omega a_2+\eta\sigma\omega+\sigma\omega a_1]}\right](\omega+\sigma\omega) > \frac{a_1a_2(\omega+\mu)[(\sigma\omega\eta+\omega a_2+\mu\sigma\omega+\omega)]}{[(1-\sigma)\omega a_2+\eta\sigma\omega+\sigma\omega a_1]} \; if \; R_0 > 1 \quad (37)$$

$$D = \mu(\omega+\mu)a_1a_2 + \frac{\beta(1-\theta q)}{N}\left[\frac{\sigma\omega}{a_2}+\frac{(1-\sigma)\omega a_2+\eta\sigma\omega}{a_1a_2}\right]\frac{\Pi}{(\omega+\mu)R_0}[R_0 - 1](\omega+\mu)a_1a_2 + \frac{\beta(1-\theta q)}{N}\left[\frac{\sigma\omega}{a_2}+\frac{(1-\sigma)\omega a_2+\eta\sigma\omega}{a_1a_2}\right]\frac{\Pi}{(\omega+\mu)R_0}[R_0 - 1]\left[\frac{a_1a_2(\omega+\mu)}{[(1-\sigma)\omega a_2+\eta\sigma\omega+\sigma\omega a_1]}\right][(1-\sigma)\omega a_1] > \frac{\beta(1-\theta q)\Pi[R_0-1][(1-\sigma)\omega a_2]}{NR_0} + \left[\frac{a_1a_2(\omega+\mu)[2\sigma\omega\eta+\omega a_2+\sigma\omega a_2+(1-\sigma)\omega a_1]}{[(1-\sigma)\omega a_2+\eta\sigma\omega+\sigma\omega a_1]}\right] \; if \; R_0 > 1 \quad (38)$$

From the Routh-Hurwitz stability criteria, all the roots of the characteristics equation (34) have negative real parts if: $A, B, C, D > 0, ABC - C^2 - A^2D > 0, and \; AB - C > 0$.

Global Stability of Endemic Equilibrium (EE) State

Theorem 3.4: The system of equations (1) – (6) has no periodic orbits.

Proof: We applied the Dulac's Criterion.

Let $X = (S, E, I_A, I, I_S, R)$. Taking the Dulac's function:

$$G = \frac{1}{SE} \quad (39)$$

we have,

$$G\frac{dS}{dt} = \frac{\Pi}{SE} - \beta(1-\theta q)\frac{(I+I_A)}{NE} - \frac{\mu}{E}$$

$$G\frac{dE}{dt} = \beta(1-\theta q)\frac{(I+I_A)}{NE} - \frac{(\omega+\mu)}{S}$$

$$G\frac{dI_A}{dt} = \frac{\sigma\omega}{S} - \frac{(\gamma+\eta+\mu+d)I_A}{SE}$$

$$G\frac{dI}{dt} = \frac{(1-\sigma)\omega}{S} + \frac{\eta I_A}{SE} - \frac{(\gamma+v+\mu+d)I}{SE}$$

$$G\frac{dI_S}{dt} = \frac{vI}{SE} - \frac{(\gamma+\mu+d)I_s}{SE}$$

$$G\frac{dR}{dt} = \frac{\gamma I_A}{SE} + \frac{\gamma I}{SE} + \frac{\gamma I_s}{SE} - \frac{\mu R}{SE}$$

Thus,

$$\frac{dGX}{dt} = \frac{\partial}{\partial S}\left(G\frac{dS}{dt}\right) + \frac{\partial}{\partial E}\left(G\frac{dE}{dt}\right) + \frac{\partial}{\partial I_A}\left(G\frac{dI_A}{dt}\right) + \frac{\partial}{\partial I}\left(G\frac{dI}{dt}\right) + \frac{\partial}{\partial I_S}\left(G\frac{dI_S}{dt}\right) + \frac{\partial}{\partial R}(G\frac{dR}{dt})$$

$$= \frac{\partial}{\partial S}\left(\frac{\Pi}{SE} - \beta(1-\theta q)\frac{(I+I_A)}{NE} - \frac{\mu}{E}\right) + \frac{\partial}{\partial E}\left(\beta(1-\theta q)\frac{(I+I_A)}{NE} - \frac{(\omega+\mu)}{S}\right) + \frac{\partial}{\partial I_A}\left(\frac{\sigma\omega}{S} - \frac{(\gamma+\eta+\mu+d)I_A}{SE}\right) + \frac{\partial}{\partial I}\left(\frac{(1-\sigma)\omega}{S} + \frac{\eta I_A}{SE} - \frac{(\gamma+v+\mu+d)I}{SE}\right) + \frac{\partial}{\partial I_S}\left(\frac{vI}{SE} - \frac{(\gamma+\mu+d)I_s}{SE}\right) + \frac{\partial}{\partial R}\left(\frac{\gamma I_A}{SE} + \frac{\gamma I}{SE} + \frac{\gamma I_s}{SE} - \frac{\mu R}{SE}\right)$$

$$= -\frac{\Pi}{S^2E} - \frac{\beta(1-\theta q)(I+I_A)}{N^2E} - \frac{(\gamma+\eta+\mu+d)}{SE} - \frac{(\gamma+v+\mu+d)}{SE} - \frac{(\gamma+\mu+d)}{SE} - \frac{\mu}{SE}$$

$$= -\left(\frac{\Pi}{S^2E} + \frac{(\gamma+\eta+\mu+d)+(\gamma+v+\mu+d)+(\gamma+\mu+d)+\mu}{SE}\right) < 0. \quad (40)$$

Hence, the systems of equation (1) - (6) has no periodic orbit. Thus proven. Since Ω is positively invariant, it follows from Poincare Bendixson theorem that all solutions of the systems of equation (1) – (6) originate and remain in Ω for all t. We conclude with the following theorem:

Theorem 3.5: The endemic equilibrium for the systems of equation is globally asymptotically stable whenever $R_0 > 1$.

Science World Journal Vol. 19(No 4) 2024 https://dx.doi.org/10.4314/swj.v19i4.31
www.scienceworldjournal.org
ISSN: 1597-6343 (Online), ISSN: 2756-391X (Print)
Published by Faculty of Science, Kaduna State University

Sensitivity Analysis

Sensitivity analysis for the basic reproduction number R_0 mainly helps to discover parameters that have a high impact on the values of R_0 and hence, it should be targeted for designing intervention strategy (Sanchez & Blower, 1997).The sensitivity analysis helps to discover the significance of the generic parameters present in the basic reproduction number R_0. The definition below is used to find the sensitivity index of each of the parameters involved in R_0.

Definition 1: Normalized Forward Sensitivity Index is differentiable with respect to a given parameter P (Chutnis *et al.,* 2008).

$$\Delta_V^{R_0} = \frac{\partial R_0}{\partial V} \cdot \frac{V}{R_0} \qquad (41)$$

The sensitivity indices of the basic reproduction number R_O with respect to the model parameters, are presented in Table 2.

Table 2: Sensitivity Indices of R_0

Parameter	Sensitivity Indices
β	1
Π	1
σ	0.00089609
θ	−0.05263158
q	−0.05263158
η	−0.00081066
d	−0.00007047
γ	−0.95596023
ω	0.00975243
μ	−1.03510029
v	−0.01753131

From table 2, the sensitivity analysis reveals that the infection transmission rate (β) has the highest positive impact on the basic reproduction number R_O. A 10% increase in β results in a corresponding 10% increase in R_O, underscoring the need to reduce the contact rates through interventions like face-mask use. Similarly, the negative index for isolation rate v indicates that increasing isolation efforts can significantly lower R_O, highlighting its importance in controlling the outbreak.

Numerical Simulations of the System

We present the numerical solutions of the model (1) – (6) for different values of the parameters to assess the impact of control strategies on the spread of the coronavirus outbreak. We conducted numerical simulations to investigate the effects of the control strategies on the transmission dynamics of COVID-19.

Parameter Estimation and Curve Fitting

We use COVID-19 cumulative confirmed cases in Kaduna State as given in Table 3 for validation of the proposed COVID-19 model and also to obtain best-fitted values of some unknown biological parameters that occur in the model. There are eleven parameters among which four are to be fitted whereas the remaining seven are estimated from literature.

From the data of confirmed COVID-19 cases in Kaduna State, we set 28th March, 2020 as the initial time with 3 confirmed cases (NCDC, 2020). The population of Kaduna State as at 2020 population estimate is put at 8,252,400 (Kaduna State Govt., 2020), so we put $N(0) = 8{,}252{,}400$ and the initial value of the Isolated class, $I_S(0) = 3$ while the value of Susceptible $S(0) = 8{,}252{,}397$ and recovered population, $R(0) = 0$. The initial values for Exposed, $E(0)$, Asymptomatic, $I_A(0)$, Symptomatic, $I(0)$, are obtained through parameter estimation.

The incubation period of COVID-19 is estimated to be 5.2 (Li *et al.,* 2020), hence $\omega = \frac{1}{5.2}$. It is reported that infectious individuals can recover within two weeks (Tang *et al.,* 2020), thus the recovery rate $\gamma = \frac{1}{14}$. The natural death rate is computed as $\mu = \frac{1}{44\times12}$ per month, where 44 years is the average life expectancy in Kaduna (Kaduna State Govt., 2020). The recruitment rate, π is calculated as $\pi = \mu \times N(0) = \frac{1}{44\times12} \times 8{,}252{,}400 = 15{,}629$ per month. The face mask compliance is estimated to be $\theta = 0.5$ (Davies et al, 2013) and the efficacy of face mask is given as $q = 0.1$ (Ngonghala *et al.,* 2020). The population of exposed individuals with no clinical symptoms of COVID-19 is estimated as $\sigma = 0.5$ (Ferguson *et al.,* 2020; Moriarty, 2020).

In addition to these estimated values, values of other parameters are mentioned in Table 2 where the parameters β (infection transmission rate), d (Disease-induced mortality rate), η (proportion of individuals who move to symptomatic class as a result of diagnosis) and v (isolation rate for symptomatic – infectious individuals) are obtained through parameter estimation technique using the least square method which is implemented by $fmincon$ routine, a part of the optimization toolbox in MATLAB software. The least-square estimation is to find the parameter values to minimize the following objective function

$$f(\phi, n) = \sum_{j=1}^{n} (I_j(t) - \widehat{I}_j(t))^2 \qquad (42)$$

where ϕ is a parameter vector to be estimated, n is the number of reported data, $\hat{I}(t)$ is the actual reported confirmed cases and $I(t)$ is the theoretical confirmed at day t.

Science World Journal Vol. 19(No 4) 2024 https://dx.doi.org/10.4314/swj.v19i4.31
www.scienceworldjournal.org
ISSN: 1597-6343 (Online), ISSN: 2756-391X (Print)
Published by Faculty of Science, Kaduna State University

Table 3: Cumulative confirmed cases of COVID-19 infection from March 2020 to June 2021

Month	March	Apr	May	June	July	Aug	Sept	Oct	Nov	Dec	Jan	Feb	March	April	May	June
Total Confirmed Case	3	35	258	766	1457	2141	2419	2655	3064	4940	7661	8476	8914	9040	9070	9121

Source: NCDC (2020)

The simulation results obtained for the COVID-19 confirmed cases in Kaduna State by fitting the proposed model (1) – (6) with the real statistics of the first 15 months from March 2020 to June 2021 are shown in Table 3. Also, Table 4 gives the values of the parameters used in the simulations.

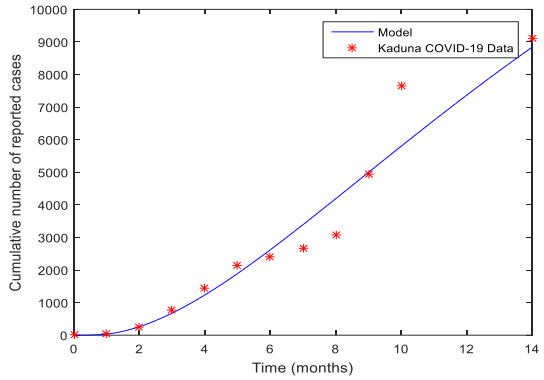

Figure 2: Model fit with the cumulative number of reported cases.

Table 4: Baseline values of the parameters of the model (1) – (6).

Parameter	Baseline Value	Reference
β	0.013280	Estimated
Π	15,629	Estimated
σ	0.5	(Ferguson et al, 2020; Moriarty
θ	0.5	(Davies et al, 2013)
q	0.1	(Ngonghala et al, 2020)
η	0.69431	Estimated
d	0.0000262	Estimated
γ	0.0714285	(Tang et al, 2020)
ω	0.1923076	(Li et al, 2020)
μ	0.0018939	(Kaduna State Govt, 2020)
v	0.001377	Estimated

The estimation of basic reproduction number for the model is given by

$$R_0 = \frac{\beta(1-\theta q)\Pi}{\mu N(\omega+\mu)}\left[\frac{\sigma\omega}{(\gamma+\eta+\mu+d)} + \frac{\eta\sigma\omega + (\gamma+\eta+\mu+d)(1-\sigma)\omega}{(\gamma+\eta+\mu+d)(\gamma+v+\mu+d)}\right] = 0.16732832 < 1 \quad (43)$$

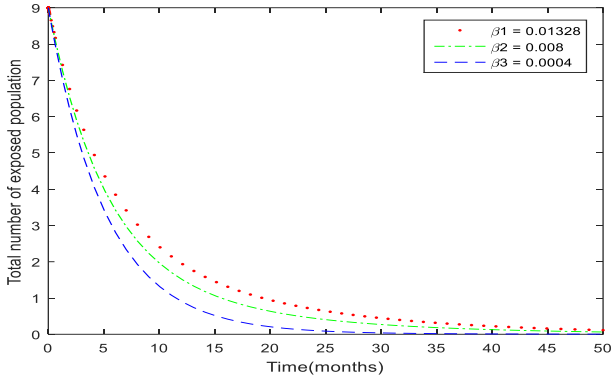

Figure 3: Dynamical behavior of exposed population for decreasing values of COVID-19 contact rate, β with no control ($\theta = q = \eta = v = 0$). Other parameter values are as in Table 4

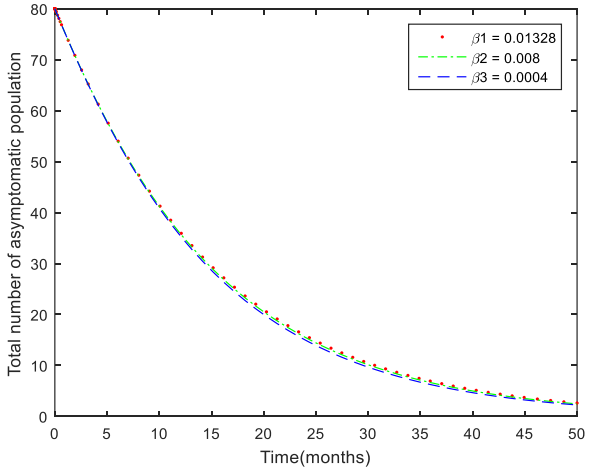

Figure 4: Dynamical behavior of asymptomatic population for decreasing values of COVID-19 contact rate, β with no control ($\theta = q = \eta = v = 0$). Other parameter values are as in Table 4

Science World Journal Vol. 19(No 4) 2024 https://dx.doi.org/10.4314/swj.v19i4.31
www.scienceworldjournal.org
ISSN: 1597-6343 (Online), ISSN: 2756-391X (Print)
Published by Faculty of Science, Kaduna State University

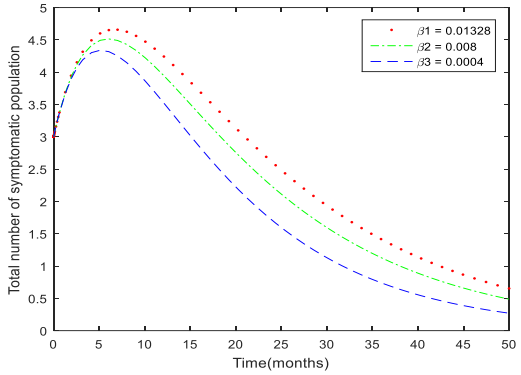

Figure 5:Dynamical behavior of symptomatic population for decreasing values of COVID-19 contact rate, β with no control $(\theta = q = \eta = v = 0)$. Other parameter values are as in Table 4

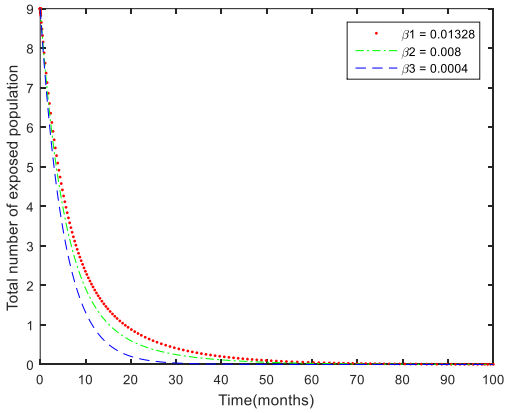

Figure 6:Dynamical behavior of exposed population for decreasing values of COVID-19 contact rate, β, with control. Other parameter values are as in Table 4

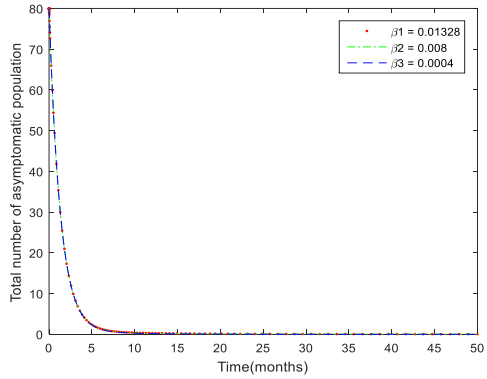

Figure 7:Dynamical behavior of asymptomatic population for decreasing values of COVID-19 contact rate, β, with control. Other parameter values are as in Table 4

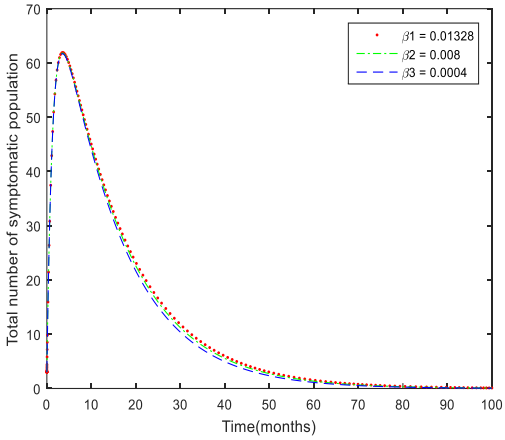

Figure 8: Dynamical behavior of symptomatic population for decreasing values of COVID-19 contact rate, β, with control. Other parameter values are as in Table 4

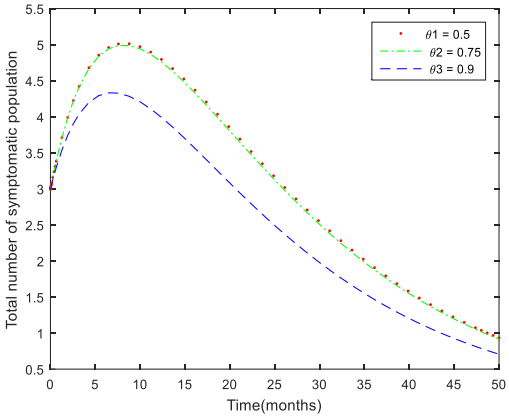

Figure 9: Effect of face masks compliance on symptomatic infectious population as a function of time, while using parameters from Table 4

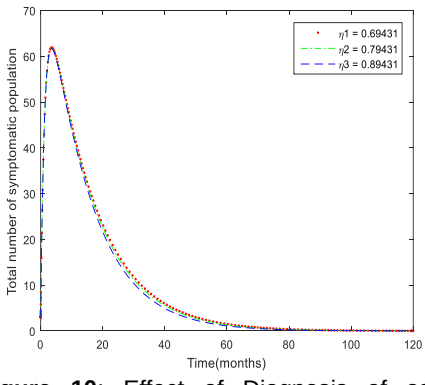

Figure 10: Effect of Diagnosis of asymptomatic individuals on the population of symptomatic individuals as a function of time without other control.

Science World Journal Vol. 19(No 4) 2024 https://dx.doi.org/10.4314/swj.v19i4.31
www.scienceworldjournal.org
ISSN: 1597-6343 (Online), ISSN: 2756-391X (Print)
Published by Faculty of Science, Kaduna State University

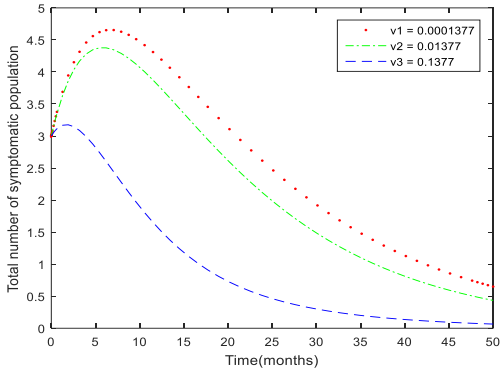

Figure 11: Effect of isolation of infectious population with no control. All other parameters are as stated in Table 4

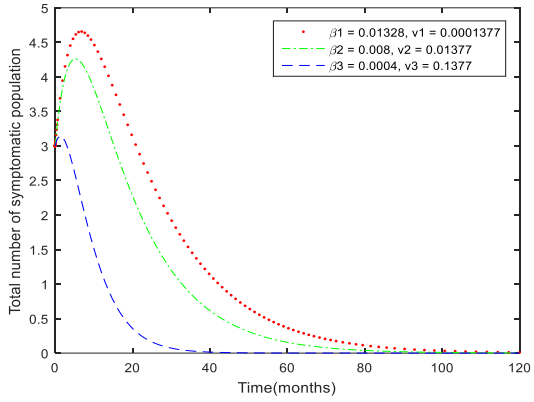

Figure 12: Dynamical behavior of symptomatic population for a decreasing value of COVID-19 contact rate, β and increasing values of isolation rate, v without other control ($\theta = q = \eta = 0$). Other parameter values are as in Table 4

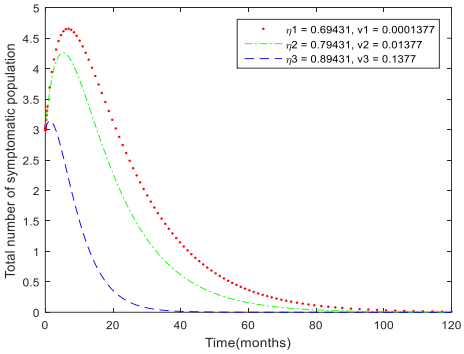

Figure 13: Effect of diagnosis and isolation without other control as a function of time. All other parameters are as stated in Table 4

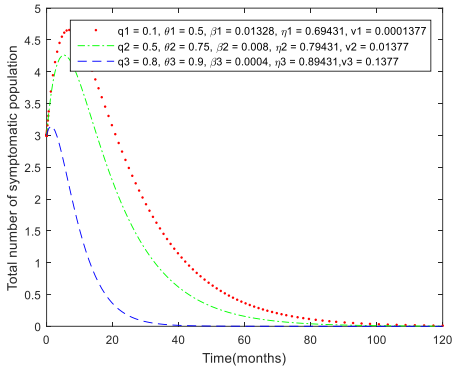

Figure 14: Dynamical behavior of symptomatic population for decreasing contact rate, increasing values of face masks compliance and efficacy, diagnosis and isolation of infectious individuals. Other parameters are as given in Table 4

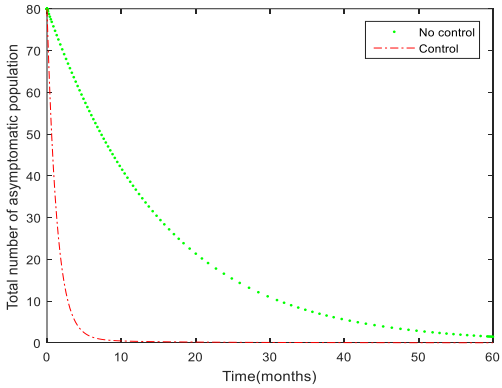

Figure 15: Dynamical behavior of asymptomatically infectious population with no control and with control.

DISCUSSION OF RESULTS

In this study, we developed a mathematical model of COVID-19 infection transmission dynamics incorporating the vital dynamics, face-mask use, asymptomatically and symptomatically-infectious individuals, clinical diagnosis of asymptomatic individuals and isolation of infected individuals taking confirmed COVID-19 data from Kaduna State, Nigeria. The model is presented in section 2. We obtained the disease-free and endemic equilibrium states of the model in section 3. The analytical and numerical results are presented as follows:

The analytical result of the model shows that the solution of the model is bounded and positively invariant. Fundamental to our analytical result is, the basic reproduction number, R_0 computed using the next-generation method and given by

$$R_0 = \frac{\beta(1-\theta q)\Pi}{\mu N(\omega+\mu)}\left[\frac{\sigma\omega}{(\gamma+\eta+\mu+d)} + \frac{\eta\sigma\omega + (\gamma+\eta+\mu+d)(1-\sigma)\omega}{(\gamma+\eta+\mu+d)(\gamma+v+\mu+d)}\right]$$

as a tool for effective disease management. Using the baseline and fitted parameter values in Table 4, the value of the basic reproduction number R_0 for Kaduna is $0.16732832 < 1$. This shows clearly that the effectiveness and coverage levels of the currently adopted public health intervention must be significantly enhanced to enable such effective control or elimination of COVID-19 infection.

The sensitivity analysis of R_0 with respect to the model parameters, was carried out using the normalized forward sensitivity indices. The results of the sensitivity index of R_0 is given in Table 2 and it shows that the more sensitive parameter is the infection transmission rate β. It is followed by the recruitment rate Π, recovery rate γ, face-mask use and compliance θ, q. The parameter β as a positive index 1 as shown in Table 2 reveals that by decreasing or increasing infection parameter will decrease or increase the basic reproduction number, R_0. Thus, efforts should be geared toward decreasing infection transmission to ensure COVID-19 disease elimination. The parameters with the negative sensitivity indices, -0.05263158; -0.01753131; -0.00081066 as shown in Table 4.1 influence reducing the disease burden in the population as their values increase.

Various numerical simulations of the model are carried out to assess the effectiveness of the various control strategies using the baseline parameter values in Table 4 and depicted in Figure $3-15$. The simulations in Figure $3-5$ shows the dynamical behavior of the population of exposed, asymptomatic and symptomatic individuals for decreasing values of contact rate with no other control measure. It shows decreasing prevalence of COVID-19 infection for decreasing infection transmission rates ($\beta = 0.01328, 0.008, 0.0004$) in the absence of face mask compliance, diagnosis of asymptomatic infectious individuals, isolation of symptomatic infectious individuals. Hence, for an effective control measure, effort should be geared at reducing the contact rate. Thus, the contact rate plays a significant role as a preventive strategy.

Figure $6-8$ shows the dynamical behavior of the population of exposed, asymptomatic and symptomatic individuals for decreasing values of contact rate ($\beta = 0.01328, 0.008, 0.0004$) with control measures ($\theta = 0.5, q = 0.1, \eta = 0.69431, v = 0.0001377$) respectively. With the basic reproduction number, $R_0 < 1$ in each case, shows the convergence of the solution profile to the disease-free equilibrium (DFE) which is consistent with Theorem 1 and Theorem 2. Figure $6-8$ further reveals that with the baseline values of face-mask use and compliance, diagnosis of asymptomatic infectious individuals, isolation of symptomatic infectious individuals, the disease can be eradicated in the shortest possible time.

Figure 9 shows the effect of face-mask compliance on symptomatic infectious population by increasing the face-mask compliance rate ($\theta = 0.5, 0.75, 0.9$) with other parameters as in Table 4. This figure reveals that increasing the use of face-mask, it reduces the number of infected individuals in the population, with the basic reproduction number, $R_0 < 1$ in each case, shows the convergence of the solution profile to the disease-free equilibrium (DFE). In Figure 10, the effect of a diagnosis of asymptomatic individuals is depicted using the baseline parameters in Table 4 by increasing the screening and diagnosis effort by 10% ($\eta = 0.69431, 0.79431, 0.89431$). The Figure shows a decrease in the proportion of infected individuals with an increasing diagnosis rate.
The effect of isolation of symptomatic infectious individuals on the dynamic of COVID-19 is simulated in Figure 11 using the baseline parameters in Table 4 by varying the isolation rate ($v = 0.0001377, 0.01377, 0.1377$). The Figure shows a decrease in the basic reproduction number with an increasing isolation rate. Thus, isolation of infected individuals can reduce the risk of future COVID-19 spread.

Figure 12 shows the dynamical behavior of symptomatic infectious individuals for a decreasing value of COVID-19 contact rate and increasing values of isolation rate without other control measures. The figure shows that by decreasing the contact rate and increasing the isolation rate simultaneously, we eliminate the COVID-19 disease burden in a possible short time. Figure 13reduces the impact of combining diagnosis of asymptomatic individuals and isolation of symptomatic individuals as an intervention strategy. As the Figure displays a decreasing number of infected individuals in the presence of increasing diagnoses of asymptomatic individuals and isolation of symptomatic individuals ($\eta = 0.69431, v = 0.0001377$; $\eta = 0.79431, v = 0.01377$; $\eta = 0.89431, v = 0.1377$).

Figure 14 shows the dynamical behavior of COVID-19 infection in the presence of decreasing contact rate, increasing values of face mask compliance and efficacy, diagnosis, and isolation of infectious individuals as control measures. It shows a decreasing number of infected individuals with the combination of all the control strategies in the model. Thus, it can be deduced from Figure 15 that the combination of decreasing contact rate, increasing values of face mask compliance and efficacy, diagnosis and isolation of infectious individuals as control measures, COVID-19 infection can be eradicated in the shortest possible time. Figure 15 shows the dynamical behavior of asymptomatic infectious individuals with no intervention strategies and with control measures. The Figure further reveals that the solution profile without control measure is consistent with Theorem 3 and Theorem 4 while the solution profile with intervention strategy is consistent with Theorem 1 and Theorem 2.

Conclusion

We developed a mathematical model of COVID-19 infection transmission to assess the impact of face-mask use & compliance, clinical diagnosis of infectious asymptomatic individuals, and isolation of infected individuals. We used confirmed COVID-19 data from Kaduna State to validate our model. Based on the findings from the study, it was evident that the infection transmission (contact) rate plays a significant role in disease management and eradication. Thus, efforts geared at reducing the contact rate will significantly eliminate the disease burden. It was further established that the basic reproduction number, R_O which serves as a threshold parameter that predicts whether an infection will spread can be used as a guide to public health or control agencies on the amount of effort needed to eradicate the disease. Finally, it was shown from the findings that a combination of face-mask use, early clinical diagnosis of asymptomatically infectious individuals, and isolation of infectious individuals is a crucial control measure against pandemics.

REFERENCES

Adewole, M.O., Onifade, A.A., Abdullah, F.A., Kasali, F., & Ismail, A.I. (2021). Modeling the dynamics of COVID-19 in Nigeria. *International Journal Applied Computation Mathematics* 7(67), 1-25. https://doi.org/10.1007/s40819-021-01014-5.

Andrea, L.B., Elisa, F., George, M., Martin, B.S., & Daniel, S. (2020). The challenges of modeling and forecasting the spread of COVID-19. *PNAS* 117(29), 16732-16738. www.pnas.org/cgi/doi/10.1073/pnas.2006520117.

Barbarossa, M.V., Fuhrmann, J., Meinke, J.H., Krieg, S., Varma, H.V., Castelletti, N., & Lippert, T. (2020). Modeling the spread of COVID-19 in Germany: Early assessment and possible scenarios. *PLOS ONE* 15(9), 1-22. https://doi.org/10.1371/jornal.pone.0238559.

Castillo-Chavez, C., Feng, Z. & Huang, W. (2002) On the Computation of R_0 and Its Role on Global Stability. In: Castillo-Chavez, P.C., Blower, S., Driessche, P., Kirschner, D. and Yakubu, A.-A., Eds., Mathematical Approaches for Emerging and Reemerging Infectious Diseases: An Introduction, Springer, Berlin, 229. https://doi.org/10.1007/978-1-4757-3667-0_13

Centers for Disease Control and Prevention (CDC). (2021). COVID-19: Isolation and quarantine. Retrieved from https://www.cdc.gov/coronavirus/2019-ncov/prevent-getting sick/quarantine-isolation.html

Centers for Disease Control and Prevention (CDC). (2022). COVID-19: How it spreads. Retrieved from https://www.cdc.gov/coronavirus/2019-ncov/your-health/how-covid-spreads.html

Chutnis, N., Hyman, J., & Cushing, J. (2008). Determining Important Parameters in the Spread of Malaria through the Sensitivity Analysis of a Mathematical Model. 7(50). https://pubmed.ncbi.nlm.nih.gov/18293044/

Danjuma, R.U., Okolo, P.N., & Dauda, M.K. (2023). Mathematical Analysis of COVID-19 Infection Model with Demographic Dynamics. 7(6). 92 – 103. https://doi.org/10.33003/fjs-2023-0706-2176

Daniel, D.O. (2020). Mathematical model for the transmission of covid-19 with nonlinear forces of infection and the need for prevention measure in Nigeria. *Journals of Infectious Diseasesand Epidemiology,* 6(5), 2474-3658. https://doi.org/10.23937/2474-3658/1510158.

Davies, A., Thompson, K.A., Giri,K., Kafatos, G., Walker, J., Bennett, A., (2013), Testing the efficacy of homemade masks: would they protect in an influenza pandemic? Disaster Medicine and Public Health Preparedness, 7, 413-418.

Diekmann, O., Heesterbeek, J. A. P., & Metz, J. A. (1990). On the definition and the computation of the basic reproduction ratio R_0 in models for infectious diseases in heterogeneous populations. *Journal of mathematical biology*, *28*(4), 365–382.

Enahoro, I., Oluwaseun, O.S., Calistus, N., & Abba B.G. (2020). Mathematical modeling and analysis of covid-19 pandemic in Nigeria. *medRxiv* 2020(1), 1-24. https://doi.org/10.1101/2020.05.22.20110387.

Ferguson, N.M., Laydon, D., Nediati-Gilani, Imai N., Ainslie, K., Baquelin, M., Bhatia, S., Boonyasiri, A., Cucunub, Z., Cuomo-Dannenburg, A.G., et al (2020), Impact of non-pharmaceutical interventions (NPIs) to reduce COVID-19 mortality and healthcare demand, London: Imperial College COVID-19 Response Team, March 16, 2020.

Firas, R., Mazhar, A., Ghena, K., Dunia, M., & Amjad, D. (2020). SARS-CoV-2 and Coronavirus Disease 2019: What We Know So Far. *Pathogens.* 9(3).

Guan, W., Ni, Z., Hu, Y., Liang, W., Ou, C., He, J., ... & Du, B. (2020). Clinical characteristics of coronavirus disease 2019 in China. *New England Journal of Medicine,* 382(18), 1708-1720.

Indwiani, A., & Ysrafil, Y. (2020). Severe Acute Respiratory Syndrome Corona Virus 2 (SARS-COV-2): An Overview of Viral Structure and Host Response. 14(4), 407 – 412. https://www.ncbi.nlm.nih.gov/pmc/articles/PMC7165108/

Kaduna State Government (2020). https://en.wikipedia.org/wiki/Kaduna_State.

Lakshmikantham, V., Leela, S. & Martynyuk, A. A. (1989). Stability Analysis of Nonlinear Systems. New York: Marcel Dekker Inc.

Li, Q, Guan, X., Wu, P., Wang, X., Zhou, L., Tong, Y., et al (2020), Early transmission dynamics in Wuhan, China, of novel coronavirus-infected pneumonia, *New England Journal of Medicine,* 382(13), 1199-1207. doi: 10.1056/NEJMoa2001316.

Moriarty, L.F. (2020), Public health responses to COVID-19 outbreaks on cruise ships-worldwide, February-March, 2020.MMWR. Morbidity and Mortality Weekly Report 69. NCDC (2020). Coronovirus (COVID-19) Highlights. https://covid19.ncdc.gov.ng.

NCDC (2021). COVID-19 Nigeria. https://covid19.ncdc.gov.ng.

Ngonghala, C.N., Iboi, E, Eikenberry, S., Scotch, M., MacIntyre, C.R., Bonds, M.H., Gumel, A.B. (2020), Mathematical assessment of the impact of non-pharmaceutical interventions on curtailing the 2019 novel coronavirus, Mathematical Biosciences, 325, 108364

Okolo, P. N., Odebode, A.G., & Dauda, M. K. (2021). A Mathematical Model of COVID-19 Infection Transmission Dynamics. KASU Journal of Mathematical Sciences (KJMS), 2(2), 57-73.

Routh-Hurwitz, A. (1964). "On The Conditions Under Which an Equation Has Only Roots with Negative Real Parts". In Bellman, Richard; Kalaba, Robert E. (eds.). Selected Papers on Mathematical Trends in Control Theory. New York: Dover.

Sanchez, M. A. & Blower, S. (1997). Uncertainty and sensitivity analysis of the basic reproductive rate. Tuberculosis as an example. Am J Epidemiol, 145(12), 1127-37.

Suleiman, A.A., Suleiman, A., Abdullahi, U.A., & Suleiman, S.A. (2021). Estimation of the case fatality rate of COVID-19 epidemiological data in Nigeria using statistical regression analysis. *Biosafety and Health,* 3,4-7. https://dx.doi.org/10.1016/j.bsheal.2020.09.003.

Tang, B., Wang, X., Li, Q., Bragazzi, N.L, Tang, S., Xiao, Y., & Wu, J. (2020). Estimation of the transmission risk of the 2019-nCoV and its implication for public health interventions, Journal of Clinical Medicine, 9, 462

Tiwari, A. (2020). Modelling and analysis of COVID-19 epidemic in India. *Journal of Safety Science and Resilience* 1, 135-140. https://doi.org/10.1016/j.jnlssr.2020.11.005.

Van den Driessche, P., & Watmough, J. (2002). Reproduction numbers and sub-threshold endemic equilibria for compartmental models of disease transmission. *Mathematical biosciences*, 180(1-2), 29-48.

World Health Organization (WHO). (2021). Pandemic. Retrieved from https://www.who.int/csr/disease/swineflu/frequently_asked_questions/pandemic/en/

WHO (2021). Impact of COVID-19 on people's livelihoods, their health and our food systems. https://www.who.int/news/item/13-10-2020-impact-of-covid-19-on-people's-livelihoods their-health-and-our-food-systems

WHO (2023). Advice for the Public: Corona Virus Disease (COVID-19). https://www.who.int/emergencies/diseases/novel-coronavirus-2019/advice-for-public

Yuliya, N.K., Konstantin, B.B., & Igor, B. (2020). Mathematical modelling of the dynamics and containment of COVID-19 in Ukraine. *Scientific Reports,* 10(19662). https://doi.org/10.1038/s41598-020-76710-1.

Yusuf, A.M., Nanshin, N., Aliyu, M., Sani, M., Dominic, M., Suleiman, M., Rilwanu, M., Suleiman, L., & Sunusi, U.U. (2020). Mathematical modelling of COVID-19 transmission and control strategies in the population of Bauchi State, Nigeria. *Annals of African Medical Research,* 3(120),37-43. https://doi.org/10.4081/aamr.2020.120.

Zhang, N., Li, Y., Huang, H., Ding, Y., Zhou, X., & Ji, Z. (2021). Airborne transmission of SARS CoV-2: The world should face the reality. *Journal of Hospital Infection,* 111,77-83. https://doi:10.1016/j.jhin.2021.05.001

Zhu, N., Zhang, D., Wang, W., Li, X., Yang, B., Song, J., ... & Niu, P. (2020). A novel coronavirus from patients with pneumonia in China, 2019. *New England Journal of Medicine,* 382(8), 727-733.